

Published in final edited form as:

Cancer Discov. 2013 May ; 3(5): 548–563. doi:10.1158/2159-8290.CD-12-0446.

Coordinate direct input of both KRAS and IGF1 receptor to activation of PI 3-kinase in KRAS mutant lung cancer

Miriam Molina-Arcas^{1,§}, David C. Hancock^{1,§}, Clare Sheridan¹, Madhu S. Kumar¹, and Julian Downward^{1,2,*}

¹Signal Transduction Laboratory, Cancer Research UK London Research Institute, 44 Lincoln's Inn Fields, London WC2A 3LY, UK

²Lung Cancer Group, Division of Cancer Biology, The Institute of Cancer Research, 237 Fulham Road, London SW3 6JB, UK

SUMMARY

Using a panel of non-small cell lung cancer (NSCLC) lines, we show here that MEK and RAF inhibitors are selectively toxic for the *KRAS* mutant genotype, while PI 3-kinase (PI3K), AKT and mTOR inhibitors are not. IGF1 receptor (IGF1R) tyrosine kinase inhibitors also show selectivity for *KRAS* mutant lung cancer lines. Combinations of IGF1R and MEK inhibitors resulted in strengthened inhibition of *KRAS* mutant lines and also showed improved effectiveness in autochthonous mouse models of *Kras* induced NSCLC. PI3K pathway activity is dependent on basal IGF1R activity in *KRAS* mutant, but not wild-type, lung cancer cell lines. *KRAS* is needed for both MEK and PI3K pathway activity in *KRAS* mutant, but not wild-type, lung cancer cells, while acute activation of *KRAS* causes stimulation of PI3K dependent upon IGF1R kinase activity. Coordinate direct input of both *KRAS* and IGF1R is thus required to activate PI3K in *KRAS* mutant lung cancer cells.

INTRODUCTION

Activating point mutations in the genes encoding the RAS subfamily of small GTP binding proteins contribute to the formation of a large proportion of human tumors. In lung cancer, one of the most prevalent cancer types worldwide (1), *KRAS* is mutationally activated in approximately 25% of adenocarcinomas (2, 3). This poses a significant therapeutic challenge, as *KRAS* mutations are generally associated with resistance to existing therapies (4, 5). Targeting RAS itself presents an attractive approach to this issue, as *RAS* mutant tumors have been shown to exhibit oncogene addiction (6, 7). However, in contrast to the efficacy of tyrosine kinase inhibitors in patients with mutant receptor tyrosine kinases (RTK), pharmacological targeting of activated RAS proteins has been unsuccessful to date. Thus, efforts have shifted towards targeting pathways acting downstream of RAS. Indeed, combined inhibition of ERK and PI3K signaling, two well-described RAS-controlled pathways, has shown some efficacy in mutant *Kras*-driven mouse lung tumor models (8). This combination of pathway inhibitory drugs is being explored in a number of early phase clinical trials, but so far both the toxicity and efficacy of this approach is unclear.

Tumors with *RAS* mutations can also show selective dependencies on activities that are not regulated directly by RAS. To identify factors or pathways necessary for survival and

*Corresponding author: julian.downward@cancer.org.uk.

§These authors contributed equally to this work

Conflict of interest: the authors have no conflicts of interest to declare.

proliferation of cells harboring *KRAS* mutations, several groups have performed synthetic lethal RNA interference (RNAi) screens. The list of candidates obtained thus far includes the TANK-binding kinase 1 (TBK1) (9), the TAK1 kinase (10), the transcription factor GATA2 (11, 12), the G1/S regulator CDK4 (13), mitotic regulators (14) and proteasome components (12, 14). Differences in cell type and in specific assay conditions may help explain some of the variability across these different datasets and deeper investigation is required in order to understand the broader significance of these factors in RAS-driven tumors. Crucially, most of these screens have identified candidate novel targets for drug development, meaning that a significant period must inevitably elapse until any such potential therapy reaches clinical trials. Thus, a complementary approach is to identify targets that are necessary for survival of *RAS* mutant cells using compounds that are already available and/or in clinical use. The use of drugs in RAS synthetic lethal screening can permit the analysis of a larger panel of cells, help avoid some of the off-target effects associated with RNA interference and, more importantly, identify immediately applicable therapeutic strategies to treat *RAS* mutant tumors.

In this study we have assayed a collection of small molecule inhibitors on a panel of human lung cancer cell lines in order to identify drugs that show selectivity for the *KRAS* mutant genotype. Cells harboring *KRAS* mutations were found to be more sensitive than *KRAS* wild-type cells to inhibition of the RAF/MEK/ERK pathway, whereas no *KRAS* genotype selectivity was observed when the PI3K/AKT/mTOR pathway was inhibited. Interestingly, however, *KRAS* mutant cells exhibit increased dependence on the activity of the IGF1R. Mechanistically, we show that the ability of KRAS to directly activate the PI3K activity of the p110 catalytic subunit requires a coordinate input from a receptor tyrosine kinase - IGF1R in the case of lung cancer - acting via the p85 regulatory subunit. These findings suggest potential therapeutic strategies for lung tumors harboring *KRAS* mutations, while avoiding the potential toxicities of direct PI3K inhibition.

RESULTS

***KRAS* mutant NSCLC cell lines are selectively sensitive to MEK, RAF and IGF1R inhibitors**

Using a collection of small molecule inhibitors we aimed to identify pathways that are critical for the maintenance and survival of tumor cells carrying an activating *KRAS* mutation, but not to those lacking this oncogene. For this purpose, we assembled a panel of twenty-five non-small cell lung cancer (NSCLC) cell lines, thirteen of which are *KRAS* mutant and twelve *KRAS* wild-type (Supplementary Table S1). Cell lines known to harbor *EGFR* mutations were purposely excluded from the selection. To conduct an initial characterization of the dependence of the two groups on expression of KRAS for cell survival, we used RNA interference to deplete endogenous levels of KRAS acutely. As anticipated, *KRAS* knockdown using two different siRNA pools led to a notable selective increase in apoptosis in most of the *KRAS* mutant, but not wild-type, cells and an accompanying decrease in cell viability (Fig. 1A-B). This effect is more statistically significant using siRNAs that have been chemically modified to reduce off-target effects (OTP (15)) and indicates that most of the *KRAS* mutant cell lines in this panel show some evidence of RAS oncogene addiction.

Next, we used the panel of twenty-five NSCLC cell lines to assess the effect on cell viability of more than fifty small molecule inhibitors targeting pathways directly controlled by RAS, such as RAF/MEK/ERK or PI3K/AKT/mTOR, as well as drugs directed against other less direct targets such as HSP90 or NF- κ B. Fig.1 (C-J) and Supplementary Fig.S1 (A-B) illustrate the effect on cell viability of several selected inhibitors. To identify those drugs achieving statistical significance in discriminating between *KRAS* mutant and wild-type cells we performed two-way ANOVA (Table 1). The analysis revealed that cells bearing

KRAS mutations tend to be, as expected (16), significantly more sensitive to RAF and MEK inhibitors than *KRAS* wild-type cells. Of the RAF inhibitors, AZ628 showed the greatest selectivity; this is a pan RAF inhibitor with somewhat more potency towards CRAF (29 nM) than BRAF (110 nM) (17). However, no significant *KRAS* genotype selectivity was observed when the PI3K/AKT/mTOR pathway was inhibited by any of a range of targeted molecules, with considerable loss of cell viability seen on most cell lines irrespective of genotype. Intriguingly, *KRAS* mutant cells exhibited enhanced sensitivity to a different class of drugs, three of the five tested IGF1R inhibitors. Indeed, p values associated with these three drugs were among the most significant, comparing favorably with those produced by the most potent MEK inhibitors. In contrast, although values failed to reach statistical significance, *KRAS* wild-type cells tended to show increased sensitivity toward EGFR inhibition compared to mutant cells. Finally, cells carrying *KRAS* mutations also responded slightly more strongly to the HSP90 inhibitors 17-AAG and 17-DMAG and to the MET/ALK kinase inhibitor PF-02341066, although the magnitude of these effects was considerably less than for the best MEK, RAF and IGF1R inhibitors. ROCK and proteasome inhibitors did not show selectivity as single agents, although combination inhibition of these pathways is selectively toxic for *KRAS* mutant cells, especially *in vivo* (11, 12). As illustrated in the viability graphs in Fig.1 and Supplementary Fig. S1, drugs directed against the same target tend to cluster together in a heat map analysis (Supplementary Fig.S1C) providing a degree of reassurance with respect to the reproducibility and on-target nature of these differential effects.

In summary, we found that NSCLC cells harboring a *KRAS* mutant allele are in general more sensitive to MEK, RAF and IGF1R inhibitors than cells with wild-type *KRAS*. No obvious differences were seen in this between the different amino acid changes at codons 12, 13 or 61 in the *KRAS* mutant cell lines used.

IGF1R inhibitors selectively inhibit AKT activation in *KRAS* mutant NSCLC cells

To investigate the mechanistic basis for the different response of NSCLC cell lines to MEK and IGF1R inhibitors, we examined the effect of these compounds on the activity of the MEK/ERK and PI3K/AKT pathways. As expected, we observed efficient reduction of ERK phosphorylation upon treatment with the MEK inhibitor PD-0325901 across the entire cell panel (Fig. 2A and Supplementary Fig. S2). In addition, there was a modest and persistent increase in AKT phosphorylation in both genotypes, probably due to suppression of well-characterized negative feedback loops (18-20). Interestingly, MEK inhibition in *KRAS* mutant, but not wild-type, cells produced a striking reduction in S6 phosphorylation, an indirect measure of mTORC1 activity, which became evident at later time points, possibly indicating a more indirect mechanism. Consistent with this finding, we also found reduced phosphorylation on Thr389 of the direct mTORC1 substrate p70S6K after MEK inhibitor treatment of *KRAS* mutant cells.

In response to IGF1R inhibition by NVP-AEW541, cells harboring a *KRAS* mutation showed an early, marked suppression of AKT phosphorylation that was sustained at 24 hours (Fig. 2B and Supplementary Fig. S3A). Consistent with this finding, there was a strong reduction in phosphorylation of the AKT substrate PRAS40 on Thr246. Notably, these effects were not evident in *KRAS* wild-type cells, even though treatment with AKT or PI3K inhibitors produced the same level of reduction in AKT phosphorylation in both *KRAS* mutant and wild-type cells (Supplementary Fig. S3B). These data suggest that inhibition of IGF1R has a clear impact upon the reduction of PI3K activity only in the cells carrying a *KRAS* mutation. Moreover, the change in AKT phosphorylation seen at 4 hours after NVP-AEW541 treatment correlated strongly with the effect on cell viability after a 72 hour treatment (Fig. 2B right panel). Thus, the differences in the reduction of AKT

phosphorylation may provide an explanation as to why *KRAS* mutant NSCLC cells are more sensitive to IGF1R inhibition.

Combining IGF1R inhibitors with MEK inhibitors enhances their differential impact upon mutant *KRAS* driven lung cancer

The data presented above demonstrate that *KRAS* mutant NSCLC cells are preferentially sensitive to inhibition of both MEK and IGF1R, and that IGF1R inhibition reduces AKT phosphorylation only in *KRAS* mutant cells. Thus, a combination of both drugs would allow for simultaneous inhibition of the PI3K/AKT and MEK/ERK pathways selectively in *KRAS* mutant cells and might be expected to increase the differential sensitivity between *KRAS* mutant and wild-type cells.

To explore this possibility we examined the effect of a combination of NVP-AEW541 with PD-0325901 upon the activity of MEK/ERK and PI3K/AKT signaling pathways after a 4 hour treatment (Fig. 2C and Supplementary Fig. S4). As expected, this combination decreased ERK phosphorylation in both mutant and wild-type cells with no differences as compared to the effect of MEK inhibitor alone. Moreover, the combination reduced AKT phosphorylation only in *KRAS* mutant cells with the effects being comparable to those seen with the IGF1R inhibitor alone. Phosphorylation on Tyr612 of the adaptor protein IRS1 served as an additional monitor of IGF1R pathway inhibition by NVP-AEW541 both alone and in combination. Intriguingly, combined inhibition of MEK and IGF1R led to a more robust inhibition of S6 phosphorylation in *KRAS* mutant cells. Consistent with this, a corresponding effect was also evident when we looked at phosphorylation of the S6 upstream kinase p70S6K. These data indicate that the combination of MEK and IGF1R inhibitors in *KRAS* mutant cells causes not only a combined inhibition of PI3K/AKT and MEK/ERK pathways, but also a stronger inhibition of mTORC1 activity.

To assess the effect of drug combinations further we augmented NVP-AEW541 with low doses of PD-0325901 and found that this reduced cell viability more strongly than single agent in *KRAS* mutant cells but not in wild-type cells (Supplementary Fig. S5A). This synergistic effect was associated with an increased induction of apoptosis, at least in some cell lines (Supplementary Fig. S5B). Comparison of the IC₆₀ values (drug dose leading to 60% survival relative to untreated cells) showed that in most *KRAS* mutant cells the combination of NVP-AEW541 with PD-0325901 clearly reduced the IC₆₀ value, whereas no significant differences were observed in most *KRAS* wild-type cells (Supplementary Fig. S6A). This increase in the differential effect between *KRAS* mutant and wild-type cells could be seen across a range of doses of NVP-AEW541 and was also evident when we compared the average response of each *KRAS* genotype (Fig. 3A). Interestingly, combination of NVP-AEW541 with low doses of the potent pan RAF inhibitor AZ628 showed similar effects (Fig. 3B). These results could be replicated with an alternative IGF1R inhibitor, OSI-906 (Supplementary Fig. S6C-E) and with trametinib (GSK1120212), an alternative MEK inhibitor (Supplementary Figs. S6B and S6F). Furthermore, the combination of IGF1R and MEK inhibitors in a long-term cell growth assay also showed a strong relative reduction of cell viability in *KRAS* mutant cells (Supplementary Fig. S6G).

Combination treatment with PI3K and MEK inhibitors has previously shown efficacy in *Kras* mutant lung tumor mouse models (8). We therefore decided to assess the effect of combining a PI3K inhibitor with low doses of a MEK or RAF inhibitor in the panel of NSCLC cell lines. Whereas treatment with PI3K inhibitors alone showed no selectivity between wild type and mutant cells, *KRAS* mutant cells exhibited enhanced sensitivity to the combination of PI3K and MEK inhibitors (Fig. 3C). Addition of a MEK or RAF inhibitor to the PI3K inhibitor GDC0941 increased the sensitivity of *KRAS* mutant but not *KRAS* wild-type cells (Fig. 3C-D and Supplementary Fig. S6H-I), but the enhanced

genotype-specific differential effect was, in general, less striking than that seen with IGF1R and MEK inhibitor combinations, due mainly to the stronger impact of direct PI3K inhibition on *KRAS* wild-type cells.

The fact that the IGF1R inhibitors used in this study are known to inhibit the closely-related Insulin receptor (INSR) to varying degrees prompted us to use siRNAs directed against IGF1R or INSR as a means to assess the effects of abrogating the activity of each receptor individually. Silencing of IGF1R expression in the panel of NSCLC cells led to a significant loss of viability of *KRAS* mutant cells as compared to *KRAS* wild-type counterparts whereas knockdown of INSR produced rather minor effects (Fig. 3E). In keeping with our observations using IGF1R inhibitors, IGF1R knockdown strikingly reduced AKT phosphorylation in *KRAS* mutant cells, with INSR silencing producing no such response (Supplementary Fig. S7A), and the combination of IGF1R knockdown with MEK inhibition augmented the *KRAS* mutant genotype-specific effect on cell viability (Fig. 3F).

To investigate the possible utility of drug combinations in an *in vivo* setting, we sought to assess the impact of MEK and IGF1R inhibition on the maintenance and progression of *Kras*-driven lung tumors in two different autochthonous genetically engineered mouse models. We elected to use trametinib for MEK inhibition due to both its potency at low concentrations *in vitro* (Fig. 1D and Supplementary Figs. S6B and S6F-G) and to its long half-life *in vivo* (21). In addition, alone of the MEK inhibitors, this drug has proven to be effective in a clinical trial, on BRAF mutant melanoma (22). Accordingly, *Kras*^{LA2-G12D/+} mice (23) were allowed to develop lung tumors that could be readily detected by micro-computerized tomography (CT) scanning. Animals were then treated daily either with vehicle, IGF1R inhibitor NVP-AEW541, MEK inhibitor trametinib or a combination of both inhibitors, for six weeks and were scanned again at the end of the treatment period. The change in volume of individual tumors over time was then evaluated. Individual lung tumors arising in *Kras*^{LA2-G12D/+} mice tend to grow relatively slowly and, as anticipated, tumors that were longitudinally tracked in vehicle control-treated animals generally exhibited a modest increase in size over the treatment period. Nevertheless, we observed that tumors in mice treated with individual MEK or IGF1R inhibitors showed a small decrease in mean tumor volume and that this effect was exacerbated when the inhibitors were combined (Fig. 3G). The efficacy of each inhibitor in this *in vivo* context is illustrated in Supplementary Fig. S7B. Analysis of individual tumor nodules at the conclusion of the treatment regime showed that IGF1R inhibition had produced a clear, albeit incomplete, reduction in AKT phosphorylation and MEK inhibition resulted in the total abrogation of ERK phosphorylation (Supplementary Fig. S7B). To evaluate the effect of MEK and IGF1R inhibition in a more aggressive *Kras*-driven mouse lung tumor model, we inoculated the lungs of *Kras*^{LSL-G12D}; *Trp53*^{Flox/Flox} mice with adenovirus expressing Cre recombinase to induce concomitant activation of oncogenic *KRAS* and deletion of the tumor suppressor p53 (24). Mice were scanned by micro-CT to identify development of individual lung tumors and tumor-bearing animals were then treated daily either with vehicle, MEK inhibitor trametinib, IGF1R inhibitor OSI-906 or a combination of both inhibitors for two weeks. After re-scanning at the end of the treatment period, changes in the volume of individual tumors over this time frame were calculated for each group (Fig. 3H). Although tumors that develop in this mouse model tend to grow more rapidly than those in the *Kras*^{LA2-G12D/+} model, we observed a similar response to MEK and IGF1R inhibition. Targeting each pathway individually provided some reduction in tumor growth but inhibiting both pathways simultaneously had a considerably stronger impact. Taken together, our results suggest the combination of IGF1R and MEK inhibitors as a novel potential therapy for *KRAS* mutant NSCLC.

***KRAS* mutant NSCLC cells exhibit increased dependence on IGF1R signaling**

The IGF1R pathway is activated by insulin-like growth factors (IGFs) binding to the heterotetrameric IGF1 receptor tyrosine kinase, resulting in receptor autophosphorylation, binding to the insulin receptor substrate (IRS) adaptor proteins, IRS protein tyrosine phosphorylation and subsequent binding to effector enzymes such as the regulatory p85 subunit of PI 3-kinase. To investigate the differential effect of IGF1R inhibition on PI3K activity in NSCLC cells we analysed the activity of the IGF1R pathway in twelve cell lines, six of which are *KRAS* mutant and six *KRAS* wild-type. Cells were serum starved overnight and then stimulated for 30 minutes with either IGF1 or EGF. A phosphospecific antibody recognizing Tyr612 of the IGF1R adaptor protein IRS1 (and also equivalent Tyr653 on IRS2) was used to measure activation of the IGF1R pathway; these sites, when phosphorylated, bind to p85, leading to PI3K activation. IGF1 stimulation induced a strong increase in phospho-IRS and phospho-AKT in all six *KRAS* mutant cell lines tested, whereas only three out of six wild-type cells showed activation of the IGF1R pathway (Fig. 4A and Supplementary Fig. S8A). As described above, cells carrying *KRAS* mutations showed a marked suppression in steady-state AKT phosphorylation in response to IGF1R inhibition by NVP-AEW541; in contrast, treatment with the EGFR inhibitor erlotinib did not affect AKT phosphorylation (Fig. 4B, Supplementary Fig. S8B). *KRAS* wild-type cells showed a higher degree of variability in their responses to IGF1R and EGFR inhibition. IGF1R inhibition decreased phospho-AKT only in the three cell lines that were responsive to IGF1 stimulation, although the magnitude of this effect was much less pronounced than in *KRAS* mutant cells. Moreover, the wild-type cells in general also showed a more prominent decrease in AKT phosphorylation in response to EGFR inhibition. In keeping with these observations, *KRAS* mutant cells generally express higher steady-state levels of phospho-IRS1, whereas *KRAS* wild-type cells have higher levels of phospho-EGFR (Supplementary Fig. S8C). To explore further the activation of PI3K in this collection of NSCLC cell lines we analysed the binding of IRS adaptor proteins to p85 α , a regulatory subunit of PI3K. Immunoprecipitation of p85 α led to the clear co-precipitation of IRS1 and/or IRS2 in the *KRAS* mutant cells whereas co-precipitation of either of these IRS proteins from *KRAS* wild-type cells was barely detectable (Figure 4C). Taken together these results suggest that cells harboring *KRAS* mutations have an IGF1R pathway with strong basal activity and that this pathway is critical for PI3K activation.

In order to assess the relative expression levels of known regulators of the IGF1R pathway between the *KRAS* mutant and wild-type genotypes, we isolated mRNA from the large NSCLC cell panel and performed quantitative PCR analysis on several components of the pathway, including the receptors (IGF1R, IGF2R, INSR), ligands (IGF1, IGF2), IGF binding proteins (IGFBPs 1-6) and adaptors (p85 α , GRB10, IRS1 and IRS2). The results showed that, whereas levels of most mRNAs are very similar across the different genotypes, *KRAS* mutant cells express modestly higher levels of IRS1 than wild-type cells. Moreover, although values do not reach statistical significance, *KRAS* mutant cells also exhibit increased levels of IRS2 (Fig. 4D and data not shown). Interestingly, analysis of publicly available gene expression data emerging from two independent large-scale cancer cell line projects (25, 26) indicates that, in general, expression levels of IRS1 are elevated in *KRAS* mutant lung cancer cell lines relative to *KRAS* wild-type comparators (Supplementary Fig. S8D-E). In addition, *KRAS* mutant lung adenocarcinoma tissue samples (27) exhibit increased expression of both IRS2 and IGF1R (Supplementary Fig. S8E). Finally, we analysed the dependence of the NSCLC cell line panel upon IRS1 and/or IRS2 expression by performing siRNA-mediated gene knockdown. Depletion of IRS1, IRS2 or both together produced a selective decrease in cell viability, accompanied by an increase in apoptosis, in the *KRAS* mutant cells that were comparable to the effects elicited by control *KRAS* siRNA treatment (Fig. 4E and see also Fig. 1A). These data are consistent with the higher degree of

sensitivity of *KRAS* mutant NSCLC cells to IGF1R inhibition by targeted small molecules and support the notion that *KRAS* mutant cells display an increased reliance upon IGF1R signaling for their survival.

KRAS depletion attenuates AKT activation in KRAS mutant NSCLC cells

To investigate whether loss of *KRAS* expression in lung cancer cells leads to the suppression of PI3K as well as ERK pathway activation, we assessed the impact of *KRAS* knockdown using two different siRNA pools in twelve cell lines, six of which are *KRAS* mutant and six *KRAS* wild-type. We observed that acute loss of *KRAS* expression led to a striking reduction in ERK phosphorylation which was much more evident in *KRAS* mutant cells. In addition, the mutant cells exhibited a similarly strong and selective reduction in S6 phosphorylation. Moreover, we found that *KRAS* depletion also significantly diminished AKT activation, monitored by phosphorylation of AKT on either Ser473 or Thr308 or PRAS40 on Thr246, preferentially in *KRAS* mutant NSCLC cells, albeit to a lesser extent than its impact upon phospho-ERK and phospho-S6 (Fig. 5A and Supplementary Fig. S9A).

The fact that mTORC1 activity, as indicated by S6 phosphorylation, is sensitive to MEK inhibition (Fig. 2A) and to *KRAS* knockdown (Fig. 5A and Supplementary Fig. S9A) in *KRAS* mutant NSCLC cells suggested that the established negative regulatory feedback loop involving phosphorylation of IRS1 by mTORC1 directly or via S6K1 (28-30) may play a significant role in the control of PI3K activity in these cells. Thus, when MEK and S6K are inhibited following *KRAS* knockdown, loss of negative feedback means there is a tendency to increase IGF1R signaling via IRS to PI3K/AKT, which counteracts any possible direct impact of *KRAS* loss on PI3K activation. We therefore sought to assess the effect of inhibiting this feedback loop upon AKT phosphorylation by treating cells with rapamycin in both the presence and absence of *KRAS* expression. As illustrated in Fig. 5B and Supplementary Fig. S9B, rapamycin treatment of control siRNA-transfected *KRAS* mutant NSCLC cells increased the levels of phospho-AKT, indicating the presence of an intact feedback loop. Nevertheless, rapamycin was clearly unable to enhance AKT activation following acute depletion of *KRAS* expression, emphasising the extent of the *KRAS* knockdown-induced decrease in AKT activation, even in cell lines such as H1792 where the effect of *KRAS* knockdown alone is less striking. Taken together these data suggest that direct interaction of *KRAS* with p110 may play a critical role in the control of PI3K signaling in NSCLC cells.

Activation of PI 3-kinase by acute oncogenic RAS signaling is sensitive to IGF1R inhibition

In order to look further into the influence of oncogenic RAS activity on IGF1R-mediated survival signaling we sought to analyse the effect of acute oncogenic RAS activation in untransformed human epithelial cells. To this end, we stably introduced a 4-hydroxytamoxifen (4-OHT)-regulatable oncogenic RAS chimeric protein, ER:HRAS V12 (31), into the spontaneously immortalised breast epithelial cell line MCF10A. Addition of 4-OHT to these cells leads to the activation of RAS downstream signaling in a time-dependent fashion, as evidenced by the sustained increase in ERK and AKT phosphorylation (Supplementary Fig. S10A). As anticipated, pre-treatment of MCF10A/ER:HRAS V12 cells with MEK inhibitors led to the abrogation of ERK phosphorylation in response to short-term 4-OHT stimulation, with no effect on AKT phosphorylation (Fig. 6A). More notably, pre-treatment of the cells with IGF1R inhibitors led to the ablation of residual and 4-OHT-inducible IRS1 phosphorylation, along with a striking inhibition of AKT phosphorylation in response to RAS activation (Fig. 6A). In order to rule out possible RAS isoform-specific effects, we first established that these observations could be replicated in the same cell system expressing a 4-OHT-activatable ER:KRAS V12 chimeric protein (10) (Supplementary Fig. S10B). Next, to extend our findings to an untransformed lung epithelial

cell context, we stably expressed ER:KRAS V12 in NL-20 (32) and Type II pneumocyte (33) cells; immortalised human cell lines derived from bronchial and alveolar epithelia respectively. Figure 6 B-C demonstrates that the short-term activation of an oncogenic KRAS signal in each of these cell lines leads to the marked increase in phosphorylation of ERK and AKT, albeit from a higher basal level than seen in the MCF10A cells. Importantly, as in the MCF10A cell background, pre-treatment of the cells with IGF1R inhibitors effectively blocks the 4-OHT-induced phosphorylation of AKT. Lastly, to investigate the acute activation of oncogenic RAS signaling in a cancer cell context, we stably expressed ER:HRAS V12 in the NSCLC cell line SK-MES-1, which is wild-type for *KRAS* and only very modestly sensitive to IGF1R inhibitors. A short 4 hour stimulation of SK-MES-1/ER:HRAS V12 with 4-OHT was also able to induce both ERK and AKT phosphorylation. Moreover, the activation of AKT was again sensitive to prior inhibition of IGF1R, although not completely blocked, whilst ERK activation remained unaffected (Fig. 6D). As demonstrated in Fig. 4B, the phosphorylation of AKT in SK-MES-1 NSCLC cells is also sensitive to inhibition of EGFR by erlotinib. We therefore assessed the effect of pre-treating SK-MES-1/ER:HRAS V12 cells with the EGFR inhibitor erlotinib, or a combination of NVP-AEW541 and erlotinib, prior to 4-OHT induction. Fig. 6D illustrates that erlotinib inhibits RAS-induced AKT activation to a similar level as NVP-AEW541, implying a significant input from EGFR as well as IGF1R in these cells. Further, the combination of both of these targeted inhibitors is able to provide near complete blockade of AKT phosphorylation in response to 4-OHT. In sum, these observations confirm that inhibition of IGF1R is able to blunt the activation of AKT elicited by acute induction of RAS signaling and further suggest that context-dependent input from other RTKs can also play a notable role. As a whole, our data support the contention that PI3K activation is controlled by coordinate input from RAS proteins and RTKs and that in *KRAS* mutant NSCLC the predominant RTK in this regard is the IGF1R (Fig. 6E).

DISCUSSION

In the standard model of RAS driven tumorigenesis, oncogenic RAS protein is thought to induce the activity of a number of downstream effector enzyme families by direct interaction of GTP-bound RAS with its targets, including RAF kinases, PI 3-kinase isoforms and guanine nucleotide exchange factors (GEFs) for RAL GTPases (4, 34). In the case of Type I PI 3-kinases, GTP-bound RAS can interact directly with the RAS-Binding Domain (RBD) on the catalytic p110 subunits (35-39), leading to enzymatic activation. The interaction of RAS.GTP with p110 promotes allosteric activation of PI 3-kinase in a manner that is cooperative with signal inputs from receptor tyrosine kinases, which act through binding of tyrosine phosphorylated sequences to the p85 regulatory subunit, relieving its autoinhibitory function (37, 38, 40). The ability of RAS to interact with p110 α has been shown to be essential for mutant *Kras*-induced lung cancer formation and mutant *Hras*-induced skin cancer formation in mouse models (41).

The ability of RAS to activate both RAF and PI3K directly has led to great interest in the possibility of treating RAS mutant tumors by inhibiting both pathways in combination. The use of PI3K and MEK inhibitors in a mouse model of *Kras*-induced lung cancer has provided support for this idea (8). However, while it has been shown that once established, RAS mutant cancers show dependence on PI 3-kinase signaling for tumor maintenance (42), it is not yet clear whether this is due to direct RAS-PI3K interaction or some more indirect mechanism. It is also not certain that *RAS* mutant cancer cells show any greater degree of dependence on PI 3-kinase signaling than do cells with other genotypes, raising the issue of whether or not PI 3-kinase inhibitors will have a useful therapeutic window in the treatment of *RAS* mutant cancers. We therefore undertook the drug screening approach described here to look for agents with selectivity for *RAS* mutant relative to *RAS* wild-type lung cancer cell

lines. The results show that while PI3K inhibition is toxic to cultured *RAS* mutant cells, it is not obviously any more selective for cells with *RAS* mutations compared to cells with other genotypes. This is in contrast to the finding that RAF/MEK/ERK pathway function is indeed selectively required by *RAS* mutant cells, as has been described with increasing certainty by others in recent years (16, 25, 26, 43, 44). In addition, we unexpectedly found that *RAS* mutant lung cancer cell lines very clearly showed heightened sensitivity to receptor tyrosine kinase inhibitors targeting the IGF1 receptor. It is worth noting that these *KRAS* mutant genotype specific effects of RAF/MEK and IGF1R inhibition are also present in data available from the Genomics of Drug Sensitivity in Cancer project from the Wellcome Trust Sanger Institute (26), based on large scale drug screening of several hundred cell lines derived from a broad range of tissue types: mutant *KRAS* selectivity is seen with AZ628 (RAF inhibitor), PD-0325901, Selumetinib and RDEA119 (MEK inhibitors), and BMS-754807 and OSI-906 (IGF1R inhibitors).

A study of *KRAS* mutant colon cancer cell lines recently reported a clear tendency towards sensitivity to IGF1R inhibition (45). In this work, as in our work on *KRAS* mutant lung cancer cell lines, *RAS* mutant cells showed good sensitivity to combinations of MEK and IGF1R inhibitors and there were indications that basal PI3K signaling was dependent on signaling flux through IGF1R to IRS1/IRS2 to p85/p110. However, while the therapeutic implications of our work and that of Ebi *et al* are similar, different mechanistic interpretations were made. In contrast to our analysis here, Ebi *et al* did not see a negative impact of removal of *KRAS* by RNAi knockdown on PI3K activity in *KRAS* mutant cells. The basis for this difference is unclear. One possibility is that it reflects the differing tissue types of origin of the cells; the frequency of coincident mutation of *KRAS* and *PIK3CA* in colon but not lung cancer suggests that there might be significant differences in the interplay between these signaling systems in the two tissues. A quantitative model of RAS signaling to PI3K concludes that the relative contributions of RAS and RTKs to PI3K activation depend strongly on the quantities and binding affinities of the interacting proteins, which are likely to vary greatly across different cell types and stimuli (46). Alternatively, this might reflect differences in the efficiency of *KRAS* knockdown between the shRNA and siRNA approaches used. It is possible that RAS protein expression has to be reduced below different thresholds to have an impact on RAF and on PI3K signaling. The tendency of MEK and mTOR inhibition to cause PI3K activation due to relief of negative feedback onto IRS1 can also obscure the direct impact of loss of RAS expression on PI3K activity, which can be revealed when mTOR activity is artificially inhibited by rapamycin, as shown in Fig. 5.

The use of a post-translationally activatable form of oncogenic RAS allows more precise probing of the role of RAS in PI3K regulation, including in a time frame that will be minimally impacted by RAS pathway induced changes in gene expression. From this, it is clear that short-term RAS activation can result in stimulation of PI3K, but that this is dependent on input from the IGF1R tyrosine kinase. It is thus likely that RAS requires relief of the inhibitory effect of the unliganded p85 regulatory subunit of PI3K (47) in order to be able to effectively activate its lipid kinase activity through direct RAS-p110 interaction, and that, in *KRAS* mutant lung cancer, this signaling input into p85 is provided by basal IGF1R signaling. This effect was seen in untransformed immortalized breast epithelial cells and also in two different cultures of normal immortalized lung epithelial cells with post-translationally inducible RAS activity. We also tested this in an NSCLC line lacking *KRAS* mutation. While this showed dependence of RAS induced PI3K pathway activation on IGF1R function, there was also a component of EGFR dependence. It is likely that this reflects the mixed IGF1R and EGFR dependence of the parental *KRAS* wild-type SK-MES-1 cell line, while the *KRAS* mutant NSCLC lines appear to be much more dependent on IGF1R rather than EGFR signaling (Fig. 4B). We speculate that in this inducible system,

acutely activated RAS will utilize input from whatever basally active RTK is present in the cells to relieve p85 mediated auto-inhibition of PI3K activity; in *KRAS* mutant NSCLC this is predominantly IGF1R, while in *KRAS* wild-type NSCLC both IGF1R and EGFR contribute.

The findings described here using cultured lung cancer cell lines and also mouse lung cancer models suggest that there may be value to the use of combinations of MEK and IGF1R inhibitors to treat *KRAS* mutant lung cancer patients. The work reported here has used small molecule kinase inhibitors that target both IGF1R and the related insulin receptor; further work will be required to determine the relative merits in this context of these inhibitors compared to IGF1R directed monoclonal antibodies, which generally do not target the insulin receptor. In comparison with PI3K inhibitors, IGF1R inhibitors appear to have less single agent impact on *KRAS* wild-type cells, suggesting that these agents might show less toxicity *in vivo*. However, to date IGF1R inhibitors have not shown great promise as single agents in clinical trials, with the exception of on some sarcomas (48). With the MEK inhibitor trametinib clearly now an attractive candidate for the treatment of *KRAS* mutant NSCLC, our work suggests that early combination with an IGF1R inhibitor may be beneficial.

EXPERIMENTAL PROCEDURES

Cell lines and culture

MCF10A/ER:HRAS V12 and SK-MES-1/ER:HRAS V12 cells were constructed by transducing parental MCF10A breast epithelial cells or SK-MES-1 NSCLC cells with a bleocin-resistant retrovirus encoding the murine ecotropic receptor. Selected cells were subsequently infected with puromycin-resistant ER:HRAS V12 retrovirus (31). MCF10A/ER:KRAS V12, NL-20/ER:KRAS V12 and TypeII/ER:KRAS V12 were constructed by transducing parental MCF10A, NL-20 or TypeII cells with pLenti-PGK-ER-KRAS(G12V) (Haber lab Addgene plasmid no. 35635) and selecting under hygromycin. Detailed origin and growing conditions of all cell lines used are given in the supplementary material. Cell lines were authenticated by the CRUK Central Cell Services facility using STR profiling.

siRNA reagents and cell viability assays

All siRNAs were obtained from Dharmacon and were used as “SMARTpools” according to the manufacturer’s instructions. Viability assays following siRNA transfection experiments or the addition of small molecule inhibitors were performed in 96-well format as previously described (12). Starting cell density was optimised to produce an 80% confluent monolayer in mock-treated cells at the conclusion of the experiment. Cell viability was determined using Cell Titer Blue (Promega) and apoptosis induction was recorded using a caspase 3/7 consensus site peptide (Z-DEVD)₂ conjugated to rhodamine 110 (Invitrogen) (12). For long-term drug treatments, cells were seeded in 12-well format for 24 h and treated with drugs for 12 days. Cells were fixed with 2% paraformaldehyde, stained with 0.2% crystal violet and finally dissolved with acetic acid. Absorbance was measured at 595 nm. Detailed information of the small inhibitors used is given in the supplementary material.

Western blotting

For quantitative western blotting, bound primary antibodies were detected by secondary conjugates compatible with infrared detection at 700nm and 800nm and membranes were scanned using the Odyssey Infrared Imaging System (Odyssey, LICOR). Alternatively, membranes were incubated with horseradish peroxidase-conjugated secondary antibody, detected using chemiluminescence (Millipore) and quantified using Image Quant LAS4000

(GE Healthcare). Detailed information of the antibodies used is given in the supplementary material.

Co-immunoprecipitations

Cells growing under steady-state conditions were scraped into ice-cold lysis buffer comprising 25 mM Tris pH 7.6, 150 mM NaCl, 0.5% Nonidet P-40, 0.5 mM DTT, 1 mM EDTA, 1 mM EGTA, 0.5 mM PMSF, 10 µg/ml leupeptin, 5 µg/ml aprotinin, 50 mM NaF, 1 mM sodium vanadate, 10 mM β-glycerophosphate and 10 mM sodium pyrophosphate. Following a short incubation on ice, lysates were centrifuged at 20,000g for 5 min at 4°C and the supernatants used for immunoprecipitation using anti-p85α antibody. Immunoprecipitates were washed three times with ice-cold lysis buffer prior to boiling in sample buffer.

Quantitative RT-PCR

RNA was isolated (Qiagen) and reverse transcription was performed (Applied Biosystems) using standard methods. Quantitative real-time PCR was performed using gene-specific primers (QuantiTect Primer Assays, Qiagen) for IGF1R, IRS1, IRS1, p85α or 18S with Fast SYBR Green Master Mix (Applied Biosystems).

Mouse experiments

KrasLSL-G12D; Trp53Flox/Flox mice and KrasLA2-G12D/+ mice were from the Mouse Models of Human Cancer Consortium (23, 49). KrasLSL-G12D; Trp53Flox/Flox mice were infected with adenovirus expressing Cre recombinase as described (50). Sixteen week-old KrasLSL-G12D; Trp53Flox/Flox mice and twelve-week-old KrasLA2-G12D/+mice were treated for two or six weeks, respectively, by oral gavage delivery of vehicle, MEK inhibitor (2.5 mg/kg/day Trametinib), IGF1R inhibitor (40 mg/kg/day OSI-906 or 50 mg/kg/day NVP-AEW541) or both drugs together. Micro-CT analysis was performed using the SkyScan 1176. Mice were scanned pre- and post-drug treatment regimes. Micro-CT data were sorted, processed and reconstructed using the N-Recon (SkyScan). Reconstructed data were subsequently imaged using DataViewer and tumor volumes were calculated using the CTan program (SkyScan).

Data analysis

Data are presented as mean ± SD unless otherwise stated. For viability and western blot quantifications, significance was assessed with the two-tailed unpaired t test. For apoptosis and gene expression analysis, significance was determined using Mann-Whitney U test. For correlation analyses Pearson's coefficient was used. Comparison between two viability curves was done using two-way ANOVA. The level of significance was set at p<0.05 *; p<0.01 **; p<0.001 ***. The CalcuSyn program (Biosoft), which employs the Combination Index equation of Chou-Talalay, was used to determine likely synergy of drug combinations using fixed drug ratios.

Supplementary Material

Refer to Web version on PubMed Central for supplementary material.

Acknowledgments

We thank Markus Diefenbacher, Ralph Fritsch, Michael Steckel, Gavin Kelly, Emma Nye and Gordon Stamp for assistance and discussion. M.M-A. is a Marie Curie Postdoctoral Fellow. This work was supported by Cancer Research UK and by the European Union Framework Programme 7 "LUNGTARGET" consortium grant.

REFERENCES

1. Ferlay J, Shin HR, Bray F, Forman D, Mathers C, Parkin DM. Estimates of worldwide burden of cancer in 2008: GLOBOCAN 2008. *Int J Cancer*. 2010; 127:2893–917. [PubMed: 21351269]
2. Ding L, Getz G, Wheeler DA, Mardis ER, McLellan MD, Cibulskis K, et al. Somatic mutations affect key pathways in lung adenocarcinoma. *Nature*. 2008; 455:1069–75. [PubMed: 18948947]
3. Heist RS, Engelman JA. SnapShot: non-small cell lung cancer. *Cancer Cell*. 2012; 21:448 e2. [PubMed: 22439939]
4. Downward J. Targeting RAS signalling pathways in cancer therapy. *Nat Rev Cancer*. 2003; 3:11–22. [PubMed: 12509763]
5. Pylayeva-Gupta Y, Grabocka E, Bar-Sagi D. RAS oncogenes: weaving a tumorigenic web. *Nat Rev Cancer*. 2011; 11:761–74. [PubMed: 21993244]
6. Torti D, Trusolino L. Oncogene addiction as a foundational rationale for targeted anti-cancer therapy: promises and perils. *EMBO Mol Med*. 2011; 3:623–36. [PubMed: 21953712]
7. Singh A, Greninger P, Rhodes D, Koopman L, Violette S, Bardeesy N, et al. A gene expression signature associated with “K-Ras addiction” reveals regulators of EMT and tumor cell survival. *Cancer Cell*. 2009; 15:489–500. [PubMed: 19477428]
8. Engelman JA, Chen L, Tan X, Crosby K, Guimaraes AR, Upadhyay R, et al. Effective use of PI3K and MEK inhibitors to treat mutant Kras G12D and PIK3CA H1047R murine lung cancers. *Nat Med*. 2008; 14:1351–6. [PubMed: 19029981]
9. Barbie DA, Tamayo P, Boehm JS, Kim SY, Moody SE, Dunn IF, et al. Systematic RNA interference reveals that oncogenic KRAS-driven cancers require TBK1. *Nature*. 2009; 462:108–12. [PubMed: 19847166]
10. Singh A, Sweeney MF, Yu M, Burger A, Greninger P, Benes C, et al. TAK1 inhibition promotes apoptosis in KRAS-dependent colon cancers. *Cell*. 2012; 148:639–50. [PubMed: 22341439]
11. Kumar MS, Hancock DC, Molina-Arcas M, Steckel M, East P, Diefenbacher M, et al. The GATA2 Transcriptional Network Is Requisite for RAS Oncogene-Driven Non-Small Cell Lung Cancer. *Cell*. 2012; 149:642–55. [PubMed: 22541434]
12. Steckel M, Molina-Arcas M, Weigelt B, Marani M, Warne PH, Kuznetsov H, et al. Determination of synthetic lethal interactions in KRAS oncogene-dependent cancer cells reveals novel therapeutic targeting strategies. *Cell research*. 2012; 22:1227–45. [PubMed: 22613949]
13. Puyol M, Martin A, Dubus P, Mulero F, Pizcueta P, Khan G, et al. A synthetic lethal interaction between K-Ras oncogenes and Cdk4 unveils a therapeutic strategy for non-small cell lung carcinoma. *Cancer Cell*. 2010; 18:63–73. [PubMed: 20609353]
14. Luo J, Emanuele MJ, Li D, Creighton CJ, Schlabach MR, Westbrook TF, et al. A genome-wide RNAi screen identifies multiple synthetic lethal interactions with the Ras oncogene. *Cell*. 2009; 137:835–48. [PubMed: 19490893]
15. Jackson AL, Burchard J, Leake D, Reynolds A, Schelter J, Guo J, et al. Position-specific chemical modification of siRNAs reduces “off-target” transcript silencing. *RNA*. 2006; 12:1197–205. [PubMed: 16682562]
16. Solit DB, Garraway LA, Pratilas CA, Sawai A, Getz G, Basso A, et al. BRAF mutation predicts sensitivity to MEK inhibition. *Nature*. 2006; 439:358–62. [PubMed: 16273091]
17. Khazak V, Astsaturov I, Serebriiskii IG, Golemis EA. Selective Raf inhibition in cancer therapy. *Expert Opin Ther Targets*. 2007; 11:1587–609. [PubMed: 18020980]
18. Chandralapaty S. Negative feedback and adaptive resistance to the targeted therapy of cancer. *Cancer Discov*. 2012; 2:311–9. [PubMed: 22576208]
19. Ma L, Chen Z, Erdjument-Bromage H, Tempst P, Pandolfi PP. Phosphorylation and functional inactivation of TSC2 by Erk implications for tuberous sclerosis and cancer pathogenesis. *Cell*. 2005; 121:179–93. [PubMed: 15851026]
20. Roux PP, Ballif BA, Anjum R, Gygi SP, Blenis J. Tumor-promoting phorbol esters and activated Ras inactivate the tuberous sclerosis tumor suppressor complex via p90 ribosomal S6 kinase. *Proceedings of the National Academy of Sciences of the United States of America*. 2004; 101:13489–94. [PubMed: 15342917]

21. Gilmartin AG, Bleam MR, Groy A, Moss KG, Minthorn EA, Kulkarni SG, et al. GSK1120212 (JTP-74057) is an inhibitor of MEK activity and activation with favorable pharmacokinetic properties for sustained in vivo pathway inhibition. *Clin Cancer Res.* 2011; 17:989–1000. [PubMed: 21245089]
22. Flaherty KT, Robert C, Hersey P, Nathan P, Garbe C, Milhem M, et al. Improved survival with MEK inhibition in BRAF-mutated melanoma. *N Engl J Med.* 2012; 367:107–14. [PubMed: 22663011]
23. Johnson L, Mercer K, Greenbaum D, Bronson RT, Crowley D, Tuveson DA, et al. Somatic activation of the K-ras oncogene causes early onset lung cancer in mice. *Nature.* 2001; 410:1111–6. [PubMed: 11323676]
24. Jackson EL, Olive KP, Tuveson DA, Bronson R, Crowley D, Brown M, et al. The differential effects of mutant p53 alleles on advanced murine lung cancer. *Cancer Res.* 2005; 65:10280–8. [PubMed: 16288016]
25. Barretina J, Caponigro G, Stransky N, Venkatesan K, Margolin AA, Kim S, et al. The Cancer Cell Line Encyclopedia enables predictive modelling of anticancer drug sensitivity. *Nature.* 2012; 483:603–7. [PubMed: 22460905]
26. Garnett MJ, Edelman EJ, Heidorn SJ, Greenman CD, Dastur A, Lau KW, et al. Systematic identification of genomic markers of drug sensitivity in cancer cells. *Nature.* 2012; 483:570–5. [PubMed: 22460902]
27. Bild AH, Yao G, Chang JT, Wang Q, Potti A, Chasse D, et al. Oncogenic pathway signatures in human cancers as a guide to targeted therapies. *Nature.* 2006; 439:353–7. [PubMed: 16273092]
28. Tzatsos A, Kandror KV. Nutrients suppress phosphatidylinositol 3-kinase/Akt signaling via raptor-dependent mTOR-mediated insulin receptor substrate 1 phosphorylation. *Mol Cell Biol.* 2006; 26:63–76. [PubMed: 16354680]
29. Harrington LS, Findlay GM, Gray A, Tolkacheva T, Wigfield S, Rebholz H, et al. The TSC1-2 tumor suppressor controls insulin-PI3K signaling via regulation of IRS proteins. *J Cell Biol.* 2004; 166:213–23. [PubMed: 15249583]
30. Shah OJ, Wang Z, Hunter T. Inappropriate activation of the TSC/Rheb/mTOR/S6K cassette induces IRS1/2 depletion, insulin resistance, and cell survival deficiencies. *Curr Biol.* 2004; 14:1650–6. [PubMed: 15380067]
31. Dajee M, Tarutani M, Deng H, Cai T, Khavari PA. Epidermal Ras blockade demonstrates spatially localized Ras promotion of proliferation and inhibition of differentiation. *Oncogene.* 2002; 21:1527–38. [PubMed: 11896581]
32. Schiller JH, Bittner G. Loss of the tumorigenic phenotype with in vitro, but not in vivo, passaging of a novel series of human bronchial epithelial cell lines: possible role of an alpha 5/beta 1-integrin-fibronectin interaction. *Cancer Res.* 1995; 55:6215–21. [PubMed: 8521416]
33. Kemp SJ, Thorley AJ, Gorelik J, Seckl MJ, O'Hare MJ, Arcaro A, et al. Immortalization of human alveolar epithelial cells to investigate nanoparticle uptake. *Am J Respir Cell Mol Biol.* 2008; 39:591–7. [PubMed: 18539954]
34. Repasky GA, Chenette EJ, Der CJ. Renewing the conspiracy theory debate: does Raf function alone to mediate Ras oncogenesis? *Trends Cell Biol.* 2004; 14:639–47. [PubMed: 15519853]
35. Kodaki T, Woscholski R, Hallberg B, Rodriguez-Viciano P, Downward J, Parker PJ. The activation of phosphatidylinositol 3-kinase by Ras. *Curr Biol.* 1994; 4:798–806. [PubMed: 7820549]
36. Rodriguez-Viciano P, Warne PH, Dhand R, Vanhaesebroeck B, Gout I, Fry MJ, et al. Phosphatidylinositol-3-OH kinase as a direct target of Ras. *Nature.* 1994; 370:527–32. [PubMed: 8052307]
37. Pacold ME, Suire S, Perisic O, Lara-Gonzalez S, Davis CT, Walker EH, et al. Crystal structure and functional analysis of Ras binding to its effector phosphoinositide 3-kinase gamma. *Cell.* 2000; 103:931–43. [PubMed: 11136978]
38. Suire S, Hawkins P, Stephens L. Activation of phosphoinositide 3-kinase gamma by Ras. *Curr Biol.* 2002; 12:1068–75. [PubMed: 12121613]
39. Yang HW, Shin MG, Lee S, Kim JR, Park WS, Cho KH, et al. Cooperative Activation of PI3K by Ras and Rho Family Small GTPases. *Molecular cell.* 2012

40. Rodriguez-Viciano P, Warne PH, Vanhaesebroeck B, Waterfield MD, Downward J. Activation of phosphoinositide 3-kinase by interaction with Ras and by point mutation. *EMBO J.* 1996; 15:2442–51. [PubMed: 8665852]
41. Gupta S, Ramjaun AR, Haiko P, Wang Y, Warne PH, Nicke B, et al. Binding of ras to phosphoinositide 3-kinase p110alpha is required for ras-driven tumorigenesis in mice. *Cell.* 2007; 129:957–68. [PubMed: 17540175]
42. Lim KH, Counter CM. Reduction in the requirement of oncogenic Ras signaling to activation of PI3K/AKT pathway during tumor maintenance. *Cancer Cell.* 2005; 8:381–92. [PubMed: 16286246]
43. McCubrey JA, Steelman LS, Abrams SL, Chappell WH, Russo S, Ove R, et al. Emerging MEK inhibitors. *Expert Opin Emerg Drugs.* 2010; 15:203–23. [PubMed: 20151845]
44. Collisson EA, Trejo CL, Silva JM, Gu S, Korkola JE, Heiser LM, et al. A Central Role for RAF->MEK->ERK Signaling in the Genesis of Pancreatic Ductal Adenocarcinoma. *Cancer Discov.* 2012; 2:685–93. [PubMed: 22628411]
45. Ebi H, Corcoran RB, Singh A, Chen Z, Song Y, Lifshits E, et al. Receptor tyrosine kinases exert dominant control over PI3K signaling in human KRAS mutant colorectal cancers. *J Clin Invest.* 2011; 121:4311–21. [PubMed: 21985784]
46. Kaur H, Park CS, Lewis JM, Haugh JM. Quantitative model of Ras-phosphoinositide 3-kinase signalling cross-talk based on co-operative molecular assembly. *The Biochemical journal.* 2006; 393:235–43. [PubMed: 16159314]
47. Kok K, Geering B, Vanhaesebroeck B. Regulation of phosphoinositide 3-kinase expression in health and disease. *Trends Biochem Sci.* 2009; 34:115–27. [PubMed: 19299143]
48. Scagliotti GV, Novello S. The role of the insulin-like growth factor signaling pathway in non-small cell lung cancer and other solid tumors. *Cancer treatment reviews.* 2012; 38:292–302. [PubMed: 21907495]
49. Jackson EL, Willis N, Mercer K, Bronson RT, Crowley D, Montoya R, et al. Analysis of lung tumor initiation and progression using conditional expression of oncogenic K-ras. *Genes & development.* 2001; 15:3243–8. [PubMed: 11751630]
50. DuPage M, Dooley AL, Jacks T. Conditional mouse lung cancer models using adenoviral or lentiviral delivery of Cre recombinase. *Nature protocols.* 2009; 4:1064–72.

SIGNIFICANCE

It has not yet been possible to target RAS proteins directly, so combined targeting of effector pathways acting downstream of RAS, including RAF/MEK and PI3K/AKT, has been the most favored approach to the treatment of *RAS* mutant cancers. This work sheds light on the ability of RAS to activate PI3K through direct interaction, indicating that input is also required from a receptor tyrosine kinase, IGF1R in the case of *KRAS* mutant lung cancer. This suggests potential novel combination therapeutic strategies for NSCLC.

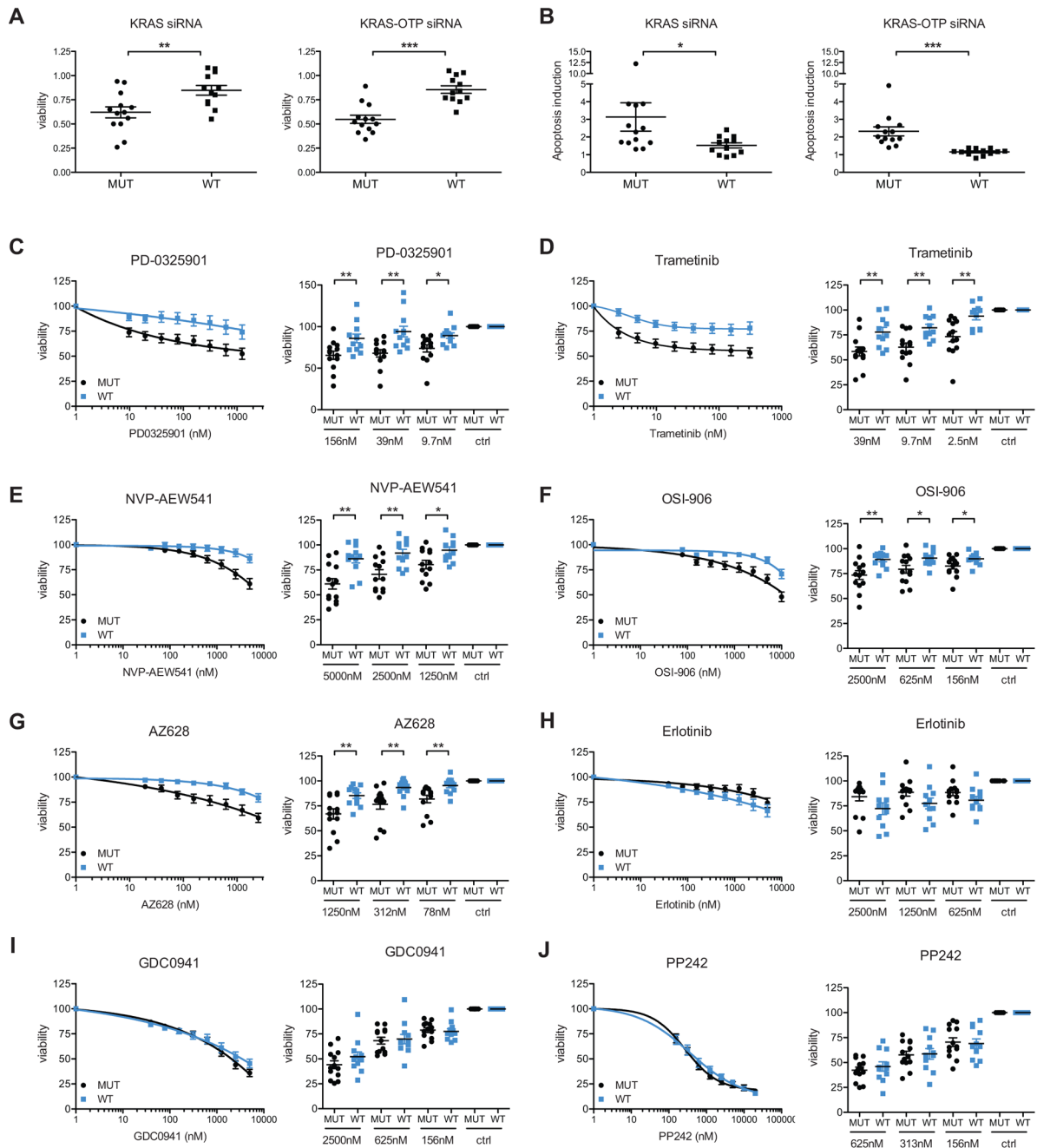


Figure 1. *KRAS* mutant NSCLC cells are selectively sensitive to MEK, RAF and IGF1R inhibitors

(A-B) Twenty-five NSCLC cell lines (thirteen *KRAS* mutant and twelve *KRAS* wild-type) were transfected with *KRAS*, *KRAS*-OTP or control siRNAs. Relative cell viability (A) and apoptosis (B) were measured 96 h after transfection.

(C-J) Twenty-five NSCLC cell lines were treated for 72 h with serial dilutions of MEK (B and C), IGF1R (E and F), RAF (G), EGFR (H), PI3K (I) and mTOR (J) inhibitors. Left panels show curves representing average values for each *KRAS* genotype (mean \pm SEM). Right panels show single data-points representing individual cell lines at three selected drug doses.

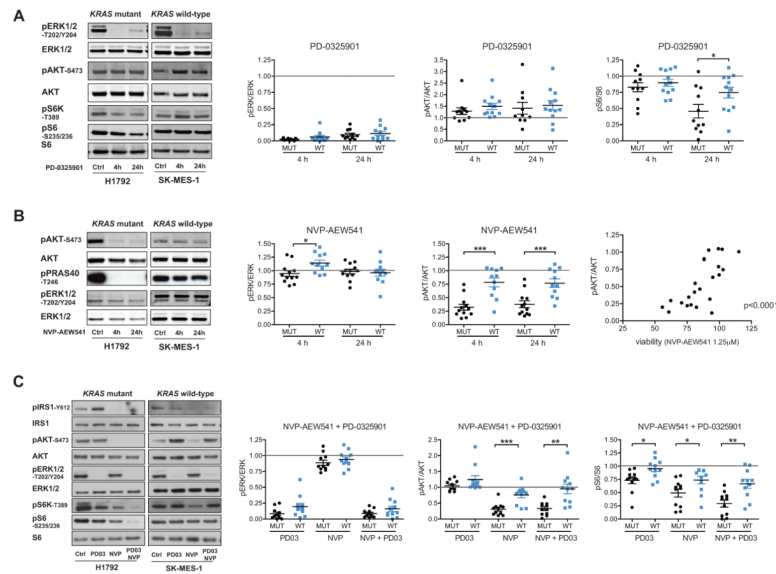


Figure 2. Effects of MEK and IGF1R inhibitors on signal transduction pathways in NSCLC cell lines

(A) *KRAS* mutant and *KRAS* wild-type NSCLC cells were treated for 4 h or 24 h with 100 nM PD-0325901 and cell lysates were probed with the indicated antibodies. For all western blots see Supplementary Figure S2.

(B) NSCLC cells were treated for 4 h or 24 h with 1 μM NVP-AEW541 and cell lysates were probed with the indicated antibodies. For all western blots see Supplementary Figure S3A. Right panel shows the correlation between pAKT/AKT ratios (at 24 h) and cell viability (measured at 72 h) after treatment with 1.25 μM NVP-AEW541.

(C) NSCLC cells were treated for 4 h with either 1 μM NVP-AEW541, 10 nM PD-0325901, or both together, and cell lysates were probed with the indicated antibodies. For all western blots see Supplementary Figure S4.

(A-C) The levels of phospho-/total ERK1/2, AKT and S6 were measured for each cell line by quantitative infrared imaging and normalized to vehicle-treated cells. H1792 and SK-MES-1 cells are displayed as exemplars of each genotype.

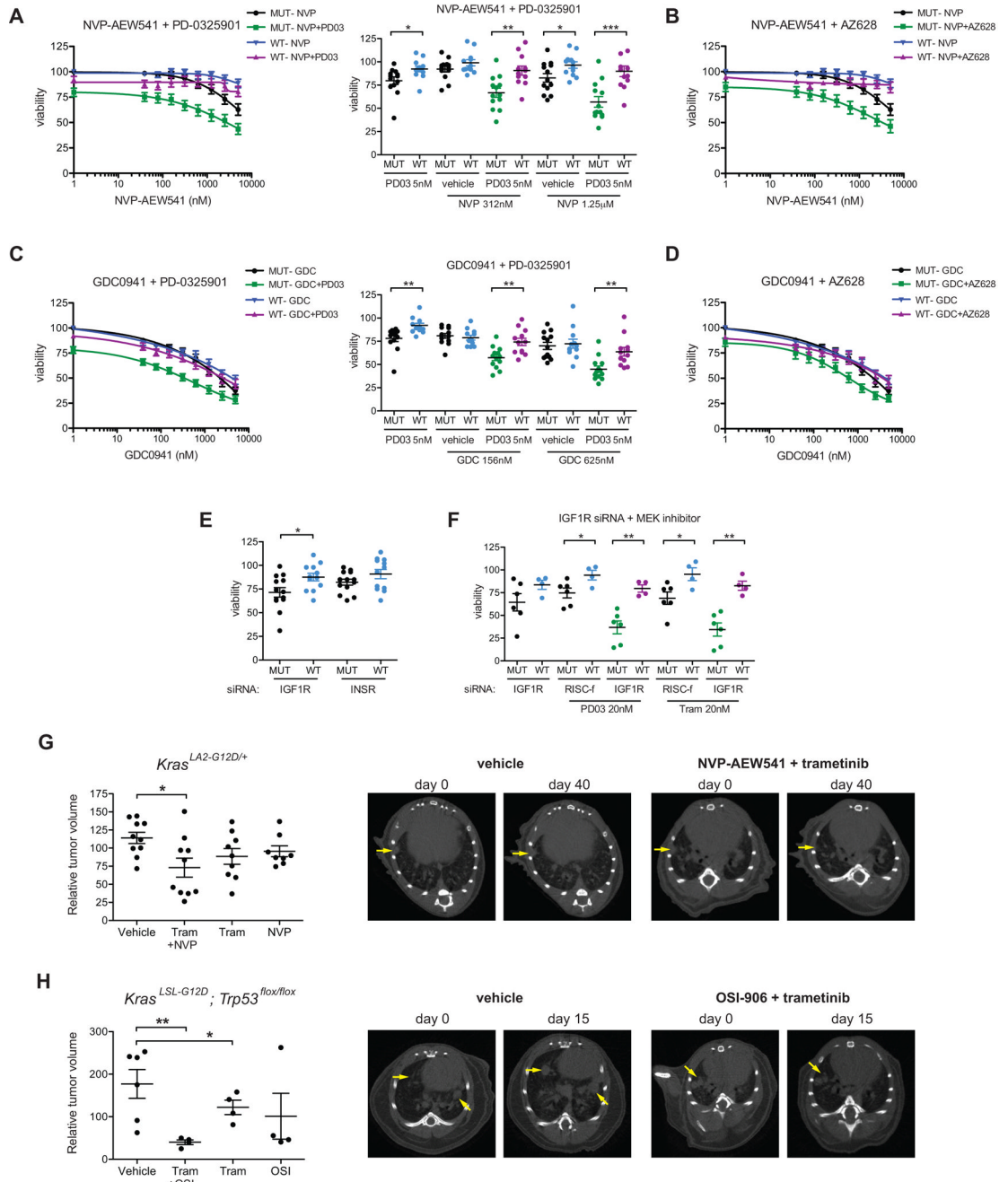


Figure 3. Combining IGF1R inhibitors with MEK or RAF inhibitors enhances the differential impact upon mutant *KRAS* cells
 (A-D) *KRAS* mutant and *KRAS* wild-type NSCLC cells were treated for 72 h with serial dilutions of IGF1R inhibitor NVP-AEW541 (A-B) or PI3K inhibitor GDC0941 (C-D), together with low doses of MEK (A and C) or RAF (B and D) inhibitor (5 nM PD-0325901 or 100 nM AZ628). Curves represent average values for each *KRAS* genotype (mean ± SEM). Right-hand panels of 3A and 3C show single data-points representing viability of individual cell lines at two representative doses of IGF1R or PI3K inhibitors in the presence or absence of MEK inhibitor PD-0325901.

- (E) Twenty-five NSCLC cell lines were transfected with IGFR, INSR or control siRNAs. Relative cell viability was measured 96 h after transfection.
- (F) Six *KRAS* mutant and four *KRAS* wild-type cells were transfected with IGFR or control siRNAs and 24 h later treated with MEK inhibitors (20 nM PD-0325901 or 20 nM trametinib). Relative cell viability was measured 72h after drug treatment.
- (G) *Kras*^{LA2-G12D/+} mice were scanned by micro-CT at twelve weeks of age to identify individual lung tumors. Animals were treated daily for six weeks either with vehicle, trametinib (2.5 mg/kg), NVP-AEW541 (50 mg/kg) or a combination of both inhibitors at these doses and then re-scanned at the end of this regime. Changes in volume of individual tumors over the treatment period were calculated for each group. Relative transaxial images before and after the treatment are shown. Yellow arrows indicate detectable lesions.
- (H) *Kras*^{LSL-G12D}; *Trp53*^{Flox/Flox} mice were infected with adenovirus expressing Cre recombinase and were scanned by micro-CT twelve weeks later to identify individual lung tumors. Animals were treated daily for two weeks either with vehicle, trametinib (2.5 mg/kg), OSI-906 (40 mg/kg) or a combination of both inhibitors at these doses and then re-scanned at the end of this regime. Changes in volume of individual tumors over the treatment period were calculated for each group. Relative transaxial images before and after the treatment are shown. Yellow arrows indicate detectable lesions.

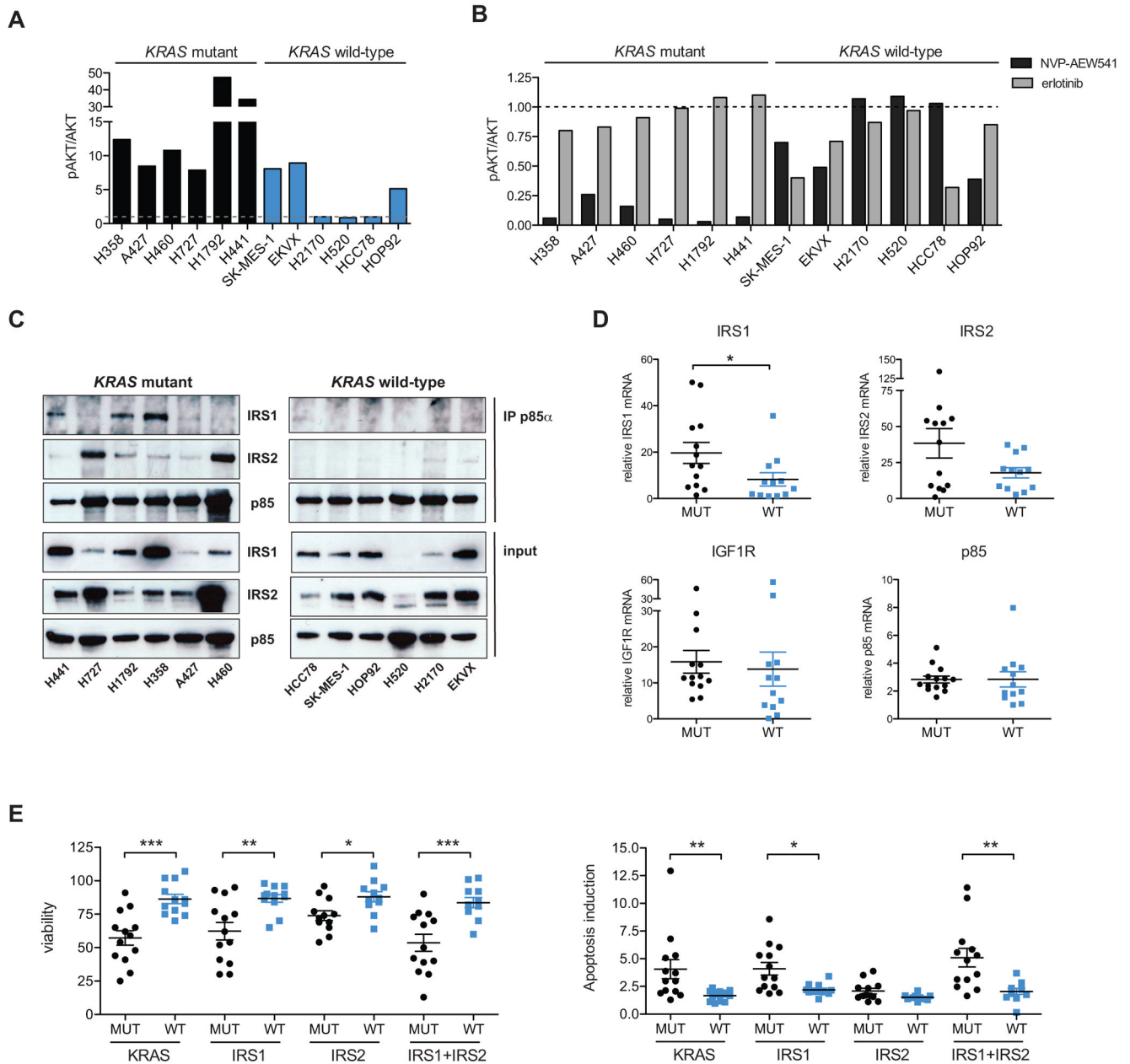


Figure 4. *KRAS* mutant NSCLC cell lines exhibit dependence upon the IGF1R pathway
 (A) Six *KRAS* mutant and six *KRAS* wild-type NSCLC cell lines were deprived of serum for 24 h and induction of phospho-/total AKT was determined following a 30 min stimulation with 20 ng/ml IGF1. For western blots see Supplementary Figure S8A.
 (B) NSCLC cell lines were treated for 4 h with either 1 μ M NVP-AEW541 or 1 μ M erlotinib and the levels of phospho-/total AKT were measured. For western blots see Supplementary Figure S8B.
 (C) Cell extracts from NSCLC cell lines growing at steady state were immunoprecipitated with anti-p85 α antibody. Immunoprecipitates and whole cell lysates were analysed by immunoblot using IRS1 and IRS2 antibodies.

(D) IRS1, IRS2, IGF1R and p85 α mRNA levels in the panel of twenty-five NSCLC cell lines were analysed by quantitative PCR. 18S RNA was used as endogenous control.

(E) Twenty-five NSCLC cell lines were transfected with KRAS, IRS1, IRS2, IRS1+IRS2 or control siRNAs. Relative cell viability and apoptosis-induction were measured 96 h after transfection.

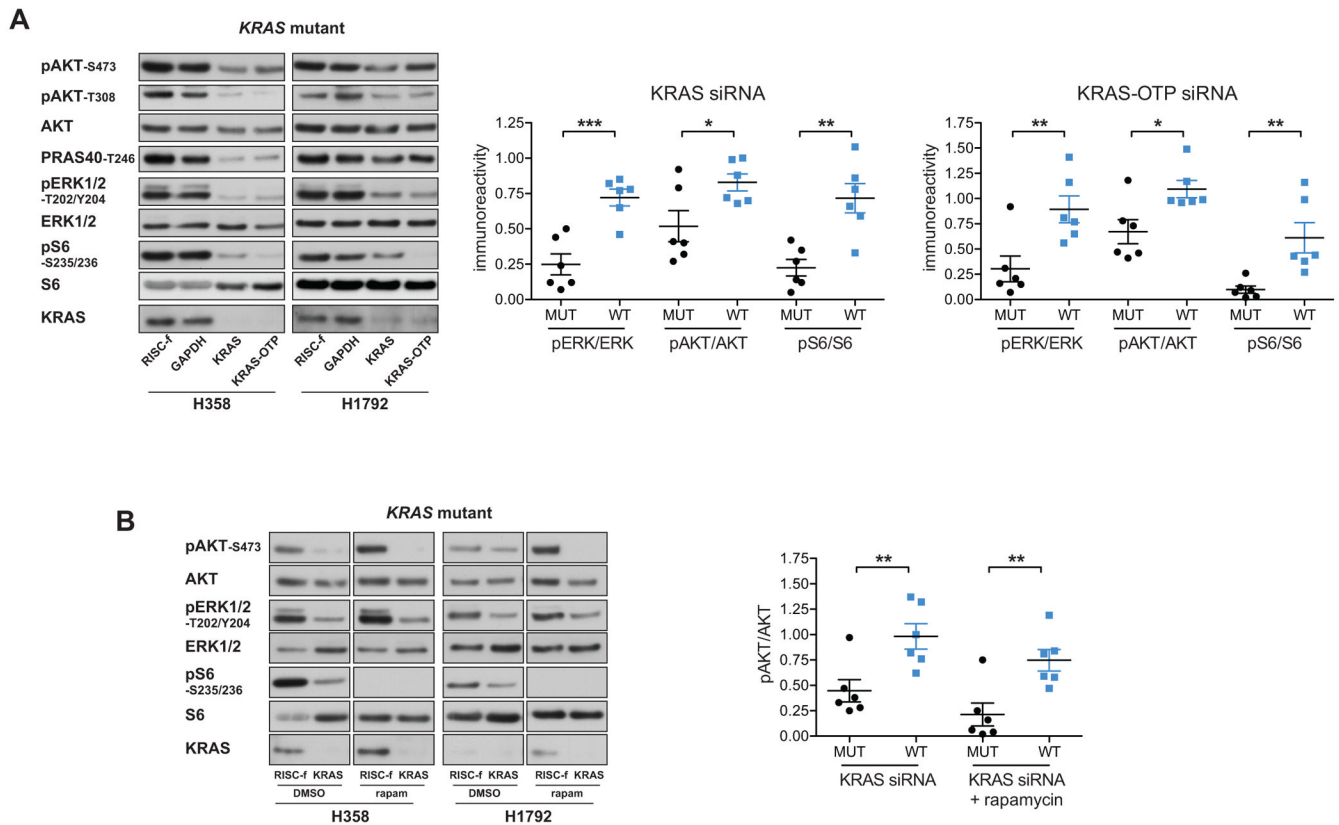


Figure 5. KRAS is required for both MEK/ERK and PI3K/AKT signaling in *KRAS* mutant NSCLC cells

(A) Six *KRAS* mutant and six *KRAS* wild-type NSCLC cell lines were transfected with *KRAS*, *KRAS*-OTP or control siRNAs for 48 h and cell lysates were probed with the indicated antibodies. The levels of phospho-/total ERK1/2, AKT and S6 were measured for each cell line and normalized to control transfected cells. H1792 and H358 cells are displayed as exemplars of the *KRAS* mutant genotype. For all western blots see Supplementary Figure S9A.

(B) NSCLC cell lines were transfected with *KRAS* or control siRNAs for 48 h. 24 h after transfection cells were treated with either DMSO or 100 nM rapamycin. Cell lysates were probed with the indicated antibodies. The level of phospho-/total AKT was measured for each cell line and normalized to control transfected cells for each condition (+/- rapamycin). H1792 and H358 cells are displayed as exemplars of the *KRAS* mutant genotype. For all western blots see Supplementary Figure S9B.

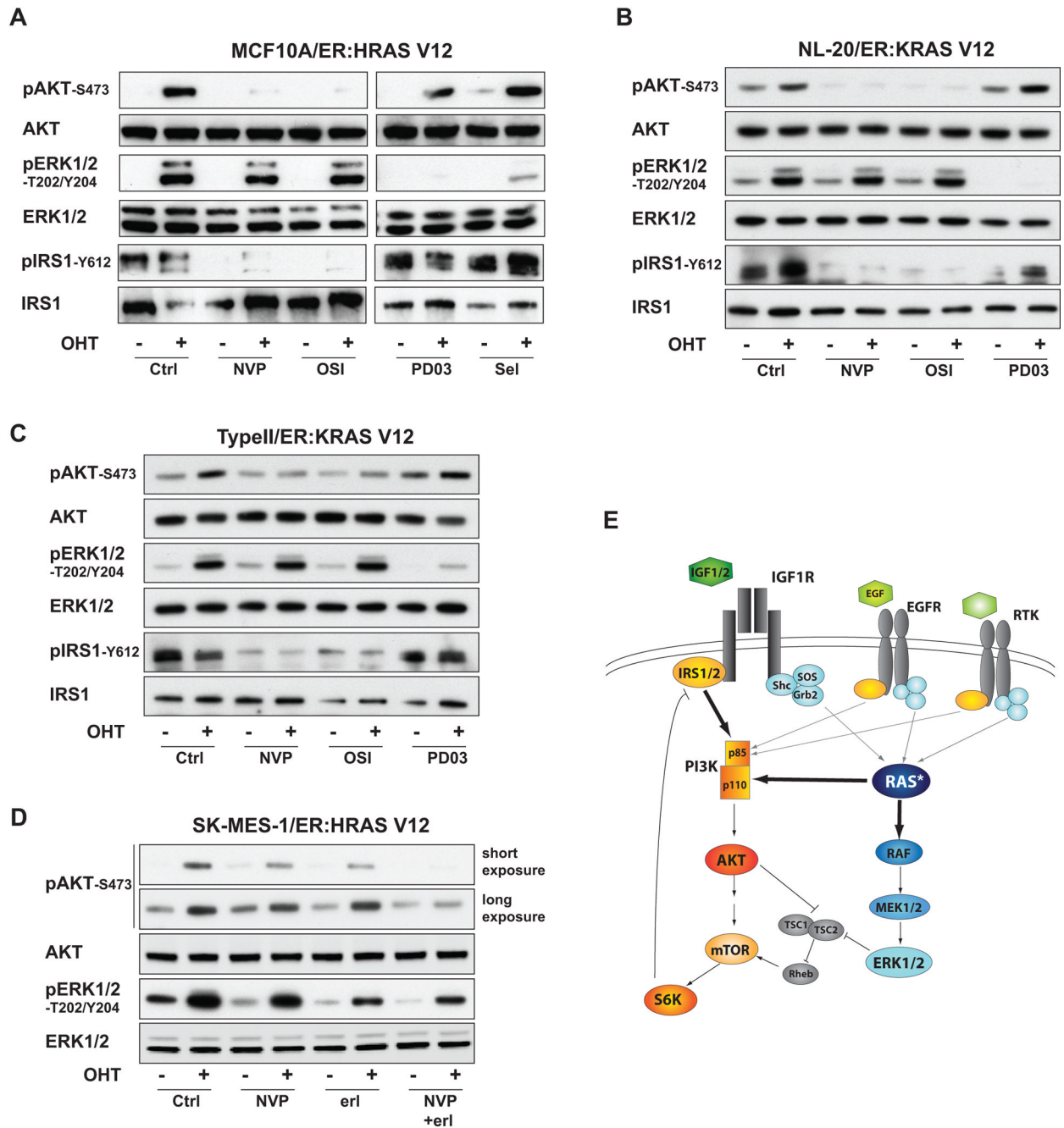


Figure 6. Acute oncogenic RAS signaling is sensitive to IGF1R inhibition

(A) MCF10A/ER:HRAS V12 cells were deprived of growth factors for 24 h and treated with vehicle or 100 nM 4-OHT for 4 h following a 20 min inhibitor pre-treatment.

(B-C) NL-20/ER:KRAS V12 (B) or Type II/ER:KRAS V12 (C) cells were deprived of serum for 24 h and treated with vehicle or 250 nM 4-OHT for 4 h following a 20 min inhibitor pre-treatment.

(D) SK-MES-1/ER:HRAS V12 cells were deprived of serum for 24 h and treated with vehicle or 100 nM 4-OHT for 4 h following a 20 min inhibitor pre-treatment.

(A-D) Inhibitor treatment: DMSO (Ctrl), 1 μ M NVP-AEW541, 1 μ M OSI-906, 5 nM PD-0325901, 90 nM Selumetinib or 1 μ M erlotinib. Cell lysates were probed with the indicated antibodies.

(E) Model of PI3K activation by oncogenic RAS and RTK signaling in *KRAS* mutant NSCLC cells.

Table 1

Drugs tested in the panel of twenty-five NSCLC cell lines

Cell viability was measured across an eight-point titration range. Two-way ANOVA was used to examine significant differences in sensitivity between *KRAS* mutant (MUT) and wild-type (WT) cells. Only primary drug targets are indicated. ns: not significant.

Drug	Target	Dose range (nM)	p-Value	significance
two-way anova (MUT vs WT)				
Trametinib	MEK	1250-9.76	0.0031	**
PD-0325901	MEK	1250-9.76	0.0053	**
Selumetinib	MEK	1250-9.76	0.0181	*
CI-1040	MEK	1250-9.76	0.0123	*
<hr/>				
AZ628	Raf	2500-19.5	0.0037	**
L779450	Raf	20000-156	0.0274	*
PLX4720	Raf	20000-156	0.0116	*
GDC-0879	Raf	20000-156	0.0483	*
Sorafenib	Raf	10000-78	0.0285	*
ZM336372	Raf	20000-156	0.0924	ns
GW5074	Raf	10000-78	0.1282	ns
SB590885	Raf	20000-156	0.2135	ns
<hr/>				
GDC0941	PI3K	5000-39	0.6078	ns
PIK-90	PI3K	2500-19.5	0.7292	ns
PIK-75	PI3K (p110a)	250-1.95	0.2477	ns
<hr/>				
NVP-BEZ235	PI3K/mTOR	250-1.95	0.2202	ns
PF-04691502	PI3K/mTOR	5000-39	0.9707	ns
<hr/>				
PI3K/AKT/mTOR				
PP242	mTOR (kinase)	20000-156	0.6741	ns
AZD8055	mTOR (kinase)	5000-39	0.5811	ns
Everolimus	mTOR (rapalog)	5000-39	0.8585	ns
Temsirolimus	mTOR (rapalog)	5000-39	0.9338	ns
Akti- 1/2	AKT	20000-156	0.2065	ns
MK-2206	AKT	20000-156	0.9727	ns

Drug	Target	Dose range (nM)	p-Value	two-way anova (MUT vs WT) significance
NVP-AEW541	IGF1R	5000-39	0.0042	**
OSI-906	IGF1R	10000-78	0.0041	**
BMS-754807	IGF1R	5000-39	0.0014	**
Picropodophyllin	IGF1R	1000-7.8	0.4921	ns
IGF-1R Inhibitor II	IGF1R	20000-156	0.5752	ns
RTK				
Erlotinib	EGFR	5000-39	0.1073	ns
Gefitinib	EGFR	5000-39	0.0139	ns
17-AAG	HSP90	500-3.9	0.0355	*
17-DMAG	HSP90	500-3.9	0.0401	*
BIB021	HSP90	500-3.9	0.1456	ns
NVP-AUY922	HSP90	500-3.9	0.5857	ns
BX-795	TBK1	5000-39	0.1786	ns
PF-02341066				
SU11274	c-Met	5000-39	0.0479	*
SU11274	c-Met	5000-39	0.4032	ns
Bortezomib	Proteasome	250-1.95	0.406	ns
MG-132	Proteasome	5000-39	0.3896	ns
PSI	Proteasome	2500-19.5	0.8714	ns
OTHER				
Doxorubicin	topoisomerase	1125-8.9	0.1158	ns
Topotecan	topoisomerase	2500-19.5	0.4927	ns
BMS-345541	IKK-b	20000-156	0.3172	ns
SC-514	IKK-2	20000-156	0.9998	ns
CAY10576	IKK-e	20000-156	0.5216	ns
5Z-7-Oxozeatenol	TAK1 (NF-KB)	20000-156	0.2505	ns
Fastudil	ROCK	20000-156	0.8516	ns
Y-27632	ROCK	20000-156	0.9011	ns
Docetaxel	microtubule	10-0.078	0.3609	ns

Drug	Target	Dose range (nM)	p-Value	two-way anova (MUT vs WT) significance
MK2a Inhibitor	MK2	5000-39	0.1352	ns
Dequalin	MT-bioenergetics	20000-156	0.7901	ns
10058-F4	c-Myc	20000-156	0.2072	ns
PF-573,228	FAK	20000-156	0.4752	ns
GDC-0449	Hedgehog pathway	20000-156	0.6057	ns
Dasatinib	SRC	5000-39	0.1236	ns